Desalination and Water Treatment
www.deswater.com

doi:10.5004/dwt.2018.22088

111 (2018) 1–11
April

Cleaning efficiency of the gas-forward osmotic backwashing in the reverse-osmosis processes for high-salinity wastewater reuse

Jun Young Park[a], Ki Tae Park[b], Minjin Kim[b], Hyung Soo Kim[b], Ji Hoon Kim[b,*]

[a]*Center of Built Environment, Sungkyunkwan University, Suwon, Korea*
[b]*Graduate School of Water Resources, Sungkyunkwan University, Suwon, Korea, Tel. +82-31-290-7647, Fax +82-31-290-7549, email: jjtt23@skku.edu*

Received 20 September 2017; Accepted 10 November 2017

ABSTRACT

This study aimed to explore the possibility of a new cleaning technique for which air flushing and forward osmotic backwashing (FOB), from among the maintenance-cleaning techniques and the reverse-osmosis (RO) processes, were combined for high-salinity wastewater reuse. Therefore, this study analyzed the cleaning efficiency in the effluent organic matter (EfOM), which is the major source of fouling for the RO membranes in terms of wastewater reuse. When non-dissolved gas and FOB are simultaneously injected into the RO membrane at a 10 % flux decline rate (FDR), the injected gas reduced the cleaning efficiency by interrupting the FOB. Although the nitrogen gas (N_2) and air did not generate bubbles via the low solubility in the FOB for which a gas-dissolved NaCl solution was used, the carbon dioxide (CO_2) generated bubbles by high-solubility showed a high cleaning efficiency. Although the pH was lowered when the CO_2 was dissolved, only a slight effect occurred in the organic-fouling cleaning; in this case, the physical effects increased the cleaning efficiency. The experiment also comprises the cleaning efficiency according to the dissolved pressure of the CO_2, and as a result, the bubble volumes was increased grew by the dissolved pressure, but the cleaning efficiency was reduced through the FOB interruption. In particular, the highest cleaning efficiency was observed at the dissolved pressure of 200 kPa because the gas/liquid ratio became 1:1.

Keywords: Forward osmotic backwashing; Gas-forward osmotic backwashing; Membrane cleaning; Organic fouling; Reverse osmosis membrane

1. Introduction

Currently, a water scarcity that is due to world-population growth, industrial development, and extreme weather is a salient concern [1,2]. Moreover, the salt concentrations in industrial and domestic wastewater have increased with industrial advancements and an increased population density [3]. High-salinity wastewater is intensively generated in coastal brackish water and factories for food, medicine, chemicals, oil refinery, and paper-making [3–6]. To solve this problem, desalination technologies such as wastewater reuse and seawater desalination have emerged [7,8]. Among them, the reverse osmosis (RO) process has rapidly developed compared to other desalination technologies, its technical maturity is high, and it is more commonly used because of the relatively low operating costs [9,10].

However, the inorganic, organic, microbial, and particulate fouling that occur in membrane processes cause problems such as a capital-expenditure increase due to the application of high-safety design factors, a concurrent increase in the operating expenditure and decrease in the operational efficiency, physicochemical membrane damage, and the deterioration of the treated water quality. Particularly, the RO process is performed without operating stop that is based on the chemical-cleaning period; therefore, contrary to microfiltration (MF) and ultrafiltration (UF), direct RO-process fouling-control cleaning methods have yet to be commercialized, and indirect fouling control through an advanced pretreatment process or cleaning in

*Corresponding author.

place (CIP) has been operated [11,12]. However, the indirect fouling control reduces operating efficiency because it is impossible to active response during operating RO process. In addition, the timing of the CIP delays decreases the cleaning efficiency due to the intensification of the irreversible fouling, and physicochemical membrane damage and secondary environmental problems can be caused [13].

Recently, studies on the application of maintenance cleaning as a direct fouling-control method that is capable of delaying the occurrence of irreversible fouling in the RO process have been conducted. Flushing uses the shear strength and turbulence from a spacer in the feed side, but it is limited because the adsorbed fouling mainly occurs at the RO membranes [14]. Studies on air flushing, wherein the shear strength is increased together with the additional turbulence that is generated by the injection-gas bubbles, have been conducted to enhance the cleaning efficiency of flushing. This is effective for the removal of the particulate fouling and biofouling even in spiral-wound RO membranes [15,16] and the efficiency of the chemical cleaning was increased [17]. Air sparging enhances the shear strength through the injection of gas during the filtration and the operation of a high flux for which the foulants are prevented from accumulating. Cui and Taha experimented with air sparging with the use of UF modules in various forms, and they confirmed that the tubular and flat membranes showed the highest operating efficiency, whereas the operating efficiencies of the hollow-fiber and spiral-wound membranes is the lowest [18].

According to the study by Ngene et al. the cleaning efficiency varied depending on the type of gas that was injected for the air flushing. In particular, carbon dioxide (CO_2)-saturated influent water showed a higher cleaning efficiency than nitrogen gas (N_2)-saturated influent water, because the solubility of CO_2 is higher than those of N_2 and air, and the CO_2 is released in the form of high-strength microbubbles when its pressure is lowered in the dissolved state [19]. Partlan performed flushing cleaning experiments to remove the RO membrane scales using feed water that had been saturated with CO_2 and dissolved under high pressure [20]. The CO_2 solution showed a higher cleaning efficiency than the N_2 saturated feed water at the pH of 3. This was confirmed because of the effects of the low pH and the shear strength from the microbubble turbulence.

Forward osmotic backwashing (FOB) is a backwashing method for which the osmotic-pressure difference between the feed and permeate waters is applicable. FOB is performed by a reduction of the operating pressure or the injection of the feed water with an osmotic pressure that is higher than the operating pressure in the RO process [21]. Contrary to the MF and UF processes, however, the cleaning efficiency is affected by the fouling characteristics and concentration polarization changes [21–25]. Additionally, the FOB cleaning efficiency decreases when the irreversible fouling increases in proportion to the operational time.

Therefore, this study additionally applied air to enhance the existing cleaning efficiency of the FOB among the maintenance cleaning techniques to control the RO process fouling for the high-salinity wastewater reuse. Based on this method, this study examined the FOB effects on the increasing of the shear strength and analyzed the cleaning efficiency changes according to the gas type and injection methods. Particularly, this study analyzed the effects depending on the injection methods and the dissolved pressure to analyze the cleaning efficiency changes according to the use of CO_2.

2. Material and methods

2.1. Feed water characteristics

In this experiment, feed water that is a replication of the treated water in the membrane-bioreactor (MBR) process of high-salinity wastewater was used. Although the efficiency of the organic matter removal in general high-salinity wastewater treatment is more than 90%, the organicmatter concentration in the feed water was maintained at 100 mg/L to minimize the effects on the decrease of the organic matter concentration in the feed water that is from the amount of organic matter that accumulates on the seawater reverse osmosis (SWRO) membrane surface. For the replication, the effluent organic matter (EfOM), humic acid (HA), sodium alginate (SA), and bovine serum albumin (BSA) were mixed at a ratio of 1:1:1. The used HA, SA, and BSA were supplied by Sigma-Aldrich, and the organic matter was filtered through a 0.45 μm filter after it was stirred in deionized water for more than 12 h. The Ca^{2+} ion was injected at 4 mM, and the total dissolved solids (TDS) concentration was finally adjusted to 20 g/L through the addition of sodium chloride (NaCl).

2.2. RO membrane

The commercialized 8 inch SWRO polyamide membrane that was used in this experiment was cut into a plate so that it could be used as a lab-scale experimental device. The cut membrane was refrigerated at 4°C through its immersion in a 1 % sodium bisulfate (SBS) solution. The SWRO membrane area that was used in this experiment is 0.0126 m^2, and a spacer was used for the feed water. The specifications of the used membrane, spacer and RO cell are given in Tables 1 and 2.

2.3. The RO unit

An exclusive RO device with a constant pressure controlling capacity regarding the cross-flow method for the series-based connection of the two RO cells, each with a membrane area of 0.0126 m^2, was the lab-scale experimental device of this study. This device consists of a 20 L feedwater tank, 20 L NaCl solution tank for the FOB, high pressure pump, water temperature controller, digital pressure gauge, and flow meter to realize the automatic and continuous operations. The permeate water and backwashing volumes were measured using an electronic scale. To prevent the high-salinity wastewater from causing corrosion, high pressure pumps, pipes, and accessories consisting of SUS-316 were used. Moreover, a relief valve was installed to control the constant pressure, and this was even possible over long time periods. The concentrated water line and permeate line were set to inflow into the feedwater tank again.

As shown in Fig. 1, for the injection of the non-dissolved gas, a gas tank was connected so that the gas could be flown into the pipe to inject the NaCl solution. A flow meter was

Table 1
Specifications of the SWRO membrane

Model	SWC5
Effective membrane area (m^2)	37.1
Permeate flow rate (m^3/d)	34.1
Stabilized salt rejection (%)	99.8
Maximum applied pressure (MPa)	8.27
Surface charge	Negative
Membrane material	Polyamide

Table 2
Specifications of the SWRO spacer and the RO cell

Geometry	Measured value
RO cell channel width, W (m)	0.095
RO cell channel height, H (m)	0.002
RO cell channel length, L (m)	0.146
Feed spacer thickness, h_{sp} (m)	0.0012
Feed spacer filament diameter, d_s (m)	0.0007
Feed spacer filament length, L_s (m)	0.004
Feed spacer filament angle, σ, (°)	90

installed to measure the flow during the injection of the NaCl solution and gas. A peristaltic pump was additionally installed to inject the NaCl solution. Pipes were installed to discharge the NaCl solution and gas in the FOB without any circulation.

Although the device configuration for the fouling is the same as the previous one for the injection NaCl solution of the dissolved gas, as shown in Fig. 2, a 24 L saturation tank was installed instead of the NaClsolution tank, and a peristaltic pump was installed to inject the NaCl solution. A pressure gauge was attached to the saturation tank to constantly check the saturation pressure.

2.4. Experimental methods and operating conditions

This experiment was performed with a constantpressurecontrol system for which the cross-flow method is employed. This experiment was also conducted with a 20 g/L salt concentration and at an operating pressure of 0.4 MPa. Before the foulants were implemented, the SWRO membrane was compacted at an operating pressure of 0.4 MPa using the deionized water for 13 h, and the conditioning was then performed for 2 h through the adjustment of the salt concentration using calcium chloride ($CaCl_2$) and NaCl. Subsequently, the fouling was caused by the injection of a total of 100 mg/L of the HA, SA, and BSA at a ratio of 1:1:1. After reaching a 10% flux decline rate (FDR), the

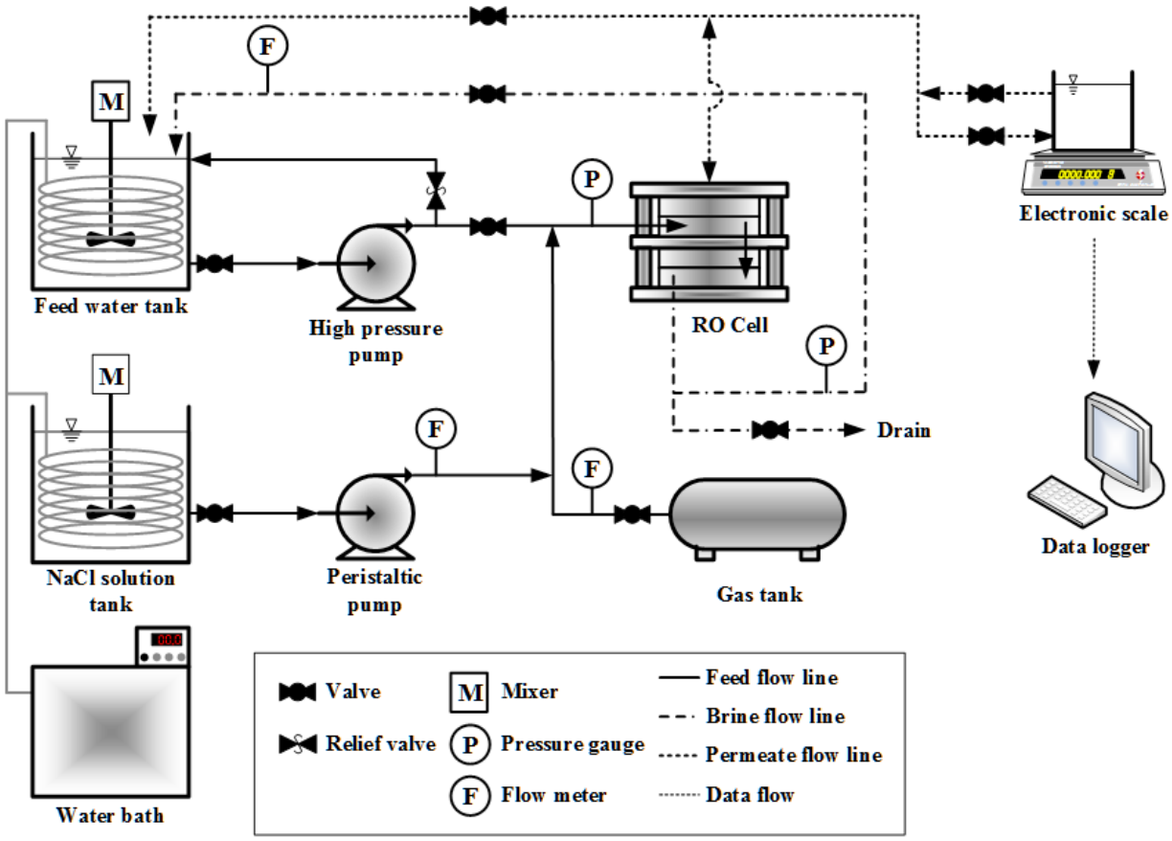

Fig. 1. Schematic diagram of the experimental device for the injection of the non-dissolved gas.

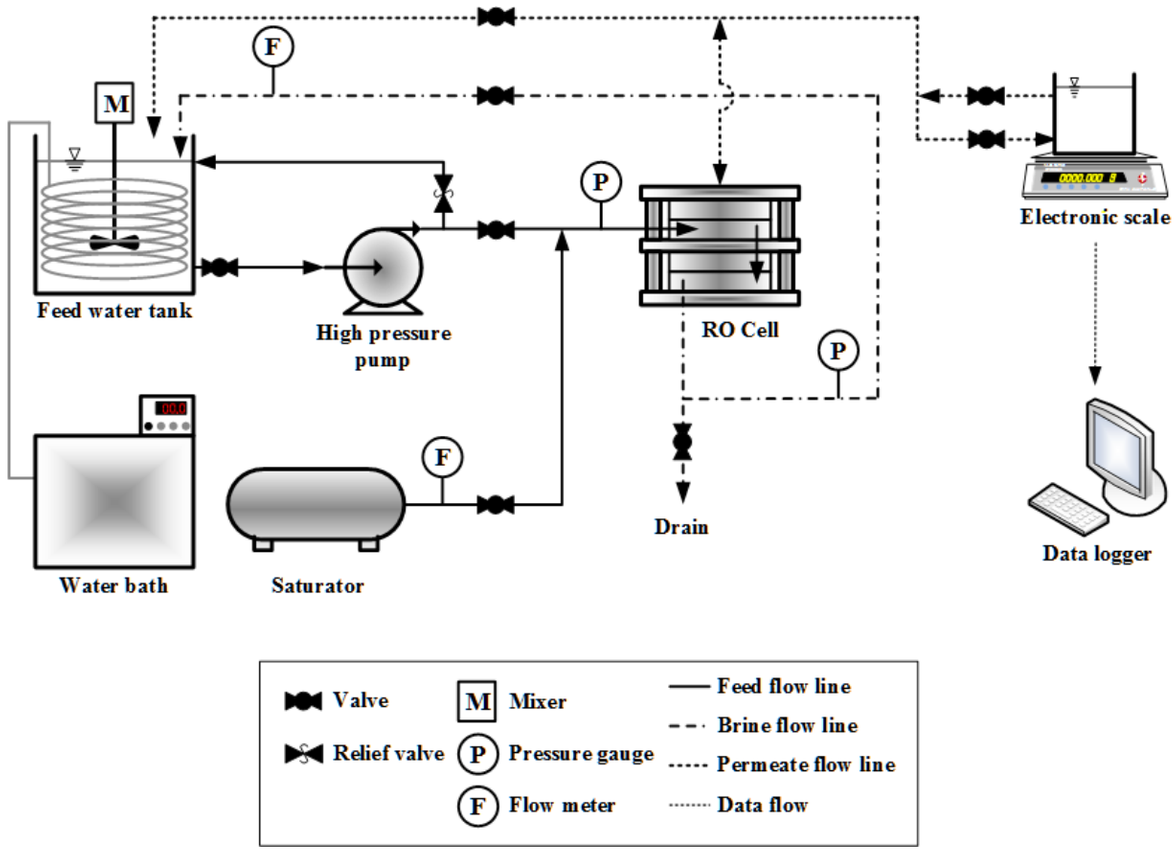

Fig. 2. Schematic diagram of the experimental device for the injection of the dissolved gas.

foulants on the membrane surface were analyzed from the separation of a single RO cell, and for another RO cell, the recovered flux was measured after FOB.

When the non-dissolved gas was injected during the cleaning, 35 g/L of each of the NaCl solution, air, N_2, and CO_2 were injected at a circulation flow rate of 0.5 L/min, while 300 mg/L of the NaCl solution was used as backwashingwater. Each of the used gases were of a 99.9% purity through a minimization of the impurities.

When the dissolved gas was injected during the cleaning, 35 g/L of each of the NaCl solution, air, N_2, and CO_2 that had been adjusted to a pH 7 in the saturation tank were added at a saturated pressure from 100 kPa to 400 kPa. Then, the FOB was performed at a circulation flow rate of 1.0 L/min, while 300 mg/L NaCl solution was used as the backwashingwater. Each of the used gases were of a 99.9% purity through a minimization of the impurities.

The temperatures of the feed water and NaCl solution were maintained at 25°C, and the room temperature in the laboratory was also maintained at 25°C to minimize the effect on the osmotic pressure, membrane permeate flux, and gas-saturation concentration that were associated with the temperature changes.

In this experiment, the resistance after the membrane compaction for which deionized water was used was defined as the membrane resistance (R_m), and the increased resistance in the conditioned state after salt pouring was defined as the salt resistance (R_{cp}). The sum of the R_m and the R_{cp} is the initial resistance and is defined as R_i. And subsequently, the resistance increased from the addition of the organic matter that was defined as the fouling resistance (R_f). The membrane resistance that was reduced by the cleaning was defined as the reversible resistance (R_r), and the membrane resistance that was not removed after the cleaning was defined as the irreversible resistance (R_{ir}). The sum of the R_i and the R_f were defined as the total resistance (R_t).

The viscosity coefficient in the fouling evaluation was determined using Eqs. (1) and (2) that were proposed by Sharqawy et al. [26], as follows:

$$\mu_{sw} = \mu_w \left(1 + A \cdot S + B \cdot S^2\right) \tag{1}$$

$$\mu_w = 4.2844 \times 10^{-5} + \left\{0.157\left(t + 64.993\right)^2 - 91.296\right\}^{-1} \tag{2}$$

where μ_{sw} is the viscosity coefficient of the feed water (Pa·s), μ_w is the viscosity coefficient of the pure water (Pa·s), S is the salinity (kg/kg), and t is the water temperature (°C), and $A = 1.541 + 1.998 \times 10^{-2}\, t - 9.51 \times 10^{-5}\, t^2$ and $B = 7.974 - 7.561 \times 10^{-2} + 4.724 \times 10^{-4}\, t^2$.

The published study of Islam and Carlson states that the coefficient of the viscosity changes when the salt and CO_2 are dissolved in water, and they presented the following empirical formula [27]:

$$\mu_{w+NaCl+CO_2} = \mu_{sw}\left(1 + 4.65x_{CO_2}{}^{1.0134}\right) \quad (3)$$

where x_{CO_2} is the mole fraction of the CO_2 in water. The FDR and cleaning efficiency were calculated as follows:

$$\text{FDR} = \left(1 - \frac{J}{J_i}\right) \times 100 \quad (4)$$

$$\text{Cleaning efficiency} = \frac{\left(J_c - J_f\right)}{\left(J_i - J_f\right)} \times 100 \quad (5)$$

where J is the reduced flux (LMH), J_0 is the initial flux (LMH), J_f is the flux of FDR 10% (LMH), and J_c is the recovered flux after FOB (LMH).

In general, a flow channel is secured by a spacer in the feed side for the RO membrane, and fouling is controlled by the formation of turbulence. In this case, the porosity of the spacer can be defined as follows [28]:

$$\varepsilon = 1 - \frac{V_{sp}}{V_{tot}} \quad (6)$$

where V_{sp} is spacer volume (m^3) and V_{tot} is total flow channel volume (m^3).

The spacer volume is associated with mesh size, filament angle, and diameter. With regard to spiral wound membranes, the angle inside diamond shape and the filament angle are both 90°. Therefore, the V_{sp} and V_{tot} can be defined as follows:

$$V_{sp} = \frac{\pi}{2} d_s^2 L_s \quad (7)$$

$$V_{tot} = HL_s^2 \quad (8)$$

where d_s is the spacer diameter (m), L_s is the spacer length (m), and H is the channel height (m). When gas and liquid are flown to the feed water at the same time, the gas/liquid ratio (θ) can be defined as follows:

$$\theta = \frac{u_G}{u_G + u_L} \quad (9)$$

where u_G and u_L are the superficial velocities of gas and liquid (m/s), respectively.

The liquid and gas superficial velocities (u_G, u_L) are corrected for the channel porosity and are calculated as follows:

$$u_G = \frac{Q_G}{3.6\left(\varepsilon \cdot W \cdot H\right)} \quad (10)$$

$$u_L = \frac{Q_L}{3.6\left(\varepsilon \cdot W \cdot H\right)} \quad (11)$$

where Q_G is the gas flow rate (L/h), Q_L is the liquid flow rate (L/h), ε is the channel porosity and W and H are the channel width and height (mm), respectively.

Unlike square spacers, the velocity of the flow direction in diamond spacers is affected by the filament angle. Therefore, given the filament angle, the velocity vector can be defined as follows [29]:

$$u_\sigma = \frac{u}{\cos\frac{\sigma}{2}} \quad (12)$$

where u_σ is velocity vector (m/s), u is u_G or u_L (m/s), and σ is filament angle (°). Wibisono reported that a higher turbulence was formed and the bubble flow was shaken more when the u_σ was larger than u [28].

2.5. Foulants extraction and analysis methods

In this experiment, the fouled membrane was cleaned by immersing it in 0.05 M NaOH solution, and it was then cleaned using an ultrasonic bath at 25°C for 1 h. Subsequently, the organic matter was extracted by neutralizing the pH using HCl. It is possible here to perform an almost perfect quantitative analysis of the organic matter on the membrane surface because the cleaning efficiency is more than 99.8 ± 0.3% under these conditions that were derived by the preliminary experiments that were conducted in the FDR 10%. The total organic carbon (TOC) value was measured using the Shimadzu TOC analyzer (TOC-L CPH), and the mean value was analyzed three times using the calibration curve of 0 mg/L to 15 mg/L.

3. Results and discussions

3..1 Cleaning efficiency according to the non-dissolved gas injection

The gas and liquid velocities were calculated using the geometrically sized RO cell and spacer, as shown in Table 1, when the FOB was performed using non-dissolved gas. As a result, the velocities are 0.0485 m/s, and the velocity vector is 0.0683 m/s.

Fig. 3 is a graph showing the cleaning efficiency and the organic-matter removal rate for each gas in the FOB. The cleaning efficiency of the flushing is 6%, while the cleaning efficiency in the existing FOB is 28.0%. In addition, the cleaning efficiencies in the FOB with the injections of the non-dissolved air, N_2, and CO_2, 24.6%, 25.5%, and 25.1%, respectively, are lower than those of the existing FOB. After the flushing, 16.2% of the organic matter was removed, and 67.6% of that was removed by the existing FOB. Moreover, the organic matter removal efficiency in the FOB with the injections of the non-dissolved air, N_2, and CO_2, 50.3%, 52.5%, and 50.7%, respectively, are lower than those of the existing FOB.

Fig. 4 is a graph showing the backwashing-water volume for each FOB gas. The backwashingwater volume in the existing FOB is 26 ml. However, the tendencies of the backwashing-water volumes in the FOB with the injections of the non-dissolved air, N_2, and CO_2, 22.2 mL, 21.4 mL, and 22.2 mL, respectively, are decreasing. It is considered that the cleaning efficiency decreased from the formation of the gas layers in the inlet of the backwashingwater because of the laminar gas flow that interrupts the FOB. Wilmarth and Ishii reported that the gas and the liquid showed the forms of separated layers when the gas and liquid flows occur concurrently in the square flow channel with a 2 mm height where the velocity for each fluid is less than 0.1 m/s

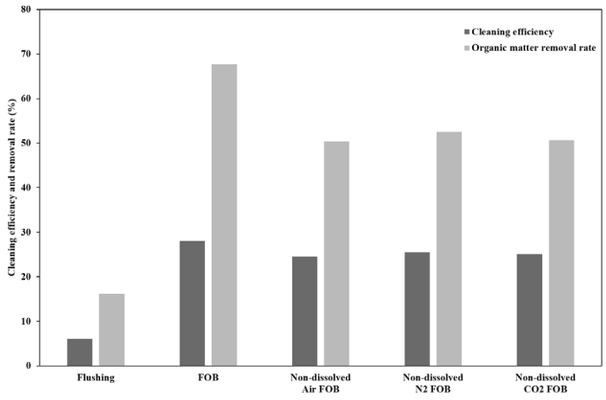

Fig. 3. Comparison of the cleaning efficiency and the organic-matter removal rate for each gas FOB with the injection of the non-dissolved gas.

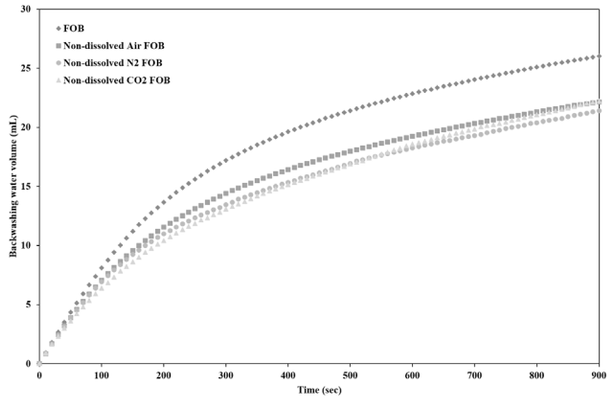

Fig. 4. Comparison of the back washing water volume for each gas FOB with the injection of the non-dissolved gas.

[30]. Moreover, Willems et al. reported that the cleaning efficiency was reduced by the channeling because the gas flowed into a low-resistance position in the spacer-filled membrane channel during the air sparging [31].

Fig. 5 is a graph showing a comparison of after FOB reversible and irreversible resistances. The ratios are 7:93 during the flushing, 30:70 during the existing FOB, 27:73 during the injection of the non-dissolved air, 29:71 during the non-dissolved N_2, and 26:74 during the non-dissolved CO_2. These ratios show a similar trend to those of the cleaning efficiency, and it was confirmed that the injection of the non-dissolved gas slightly reduced the cleaning efficiency.

3.2. Cleaning efficiency according to the dissolved gas injection

In this experiment, the dissolved air, N_2, and CO_2 were analyzed regarding the FOB cleaning efficiencies. In addition, the pH was reduced to approximately 3.9 during the saturation of the CO_2 at a pressure of 100 kPa. To evaluate the effect of the cleaning efficiency on the pH, a NaCl solution at a pH of 3.9 was additionally used in the N_2 saturation.

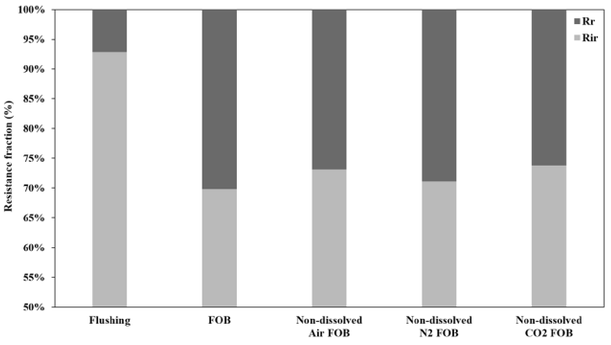

Fig. 5. Comparison of after FOB reversible and irreversible resistances for each gas with the injection of the non-dissolved gas.

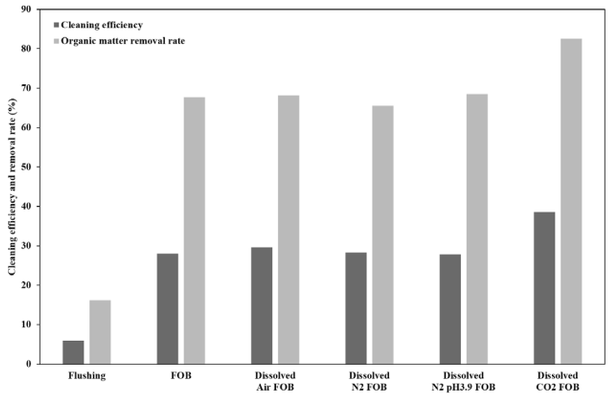

Fig. 6. Comparison of the cleaning efficiency and organic matter removal rate for each gas of the FOB with the dissolved-gas injection.

Fig. 6 is a graph showing the cleaning efficiency and organic matter removal rate for each dissolved gas in the FOB. The cleaning efficiencies of the FOB with the injections of the dissolved air and N_2 are similar to those of the existing FOB, 29.6%, and 28.3%, respectively. In addition, the cleaning efficiency of the FOB with the injection of the dissolved N_2 solution at a pH of 3.9 is 27.9%. As a result, it was confirmed that the cleaning efficiency did not affect the pH.

Alternatively, the cleaning efficiency of the FOB with the injection of the dissolved CO_2 solution is higher than that of the existing FOB, 38.6%. It is considered that the cleaning efficiency increased because the microbubbles were generated in the CO_2saturated solution, unlike the air and N_2 saturated solutions.

The CO_2 solubility is 0.034 mol/L at 25°C and 1 atm, and it is considerably higher than those of O_2 and N_2, 0.0013 mol/L and 0.00061 mol/L, respectively. CO_2 mostly exists in water in the molecular state because of the low hydration equilibrium constant. Therefore, unlike air and N_2, microbubbles are generated to increase the cleaning efficiency because the dissolved CO_2 is discharged by the pressure difference. According to the study by Ngene et al., the cleaning efficiency varies depending on the type of gas that is injected in the air flushing. In particular, CO_2 saturated

influent water showed a higher cleaning efficiency than N_2 saturated influent water. They reported that CO_2 has a high shear strength because it remained in the molecular state when its microbubbles formed [19].

Partlan performed cleaning experiments to remove the scale on the RO membranes with flushing using feed water that had been saturated with dissolved CO_2 under a high pressure [20]. Then, he compared the cleaning efficiency with feed water that had been saturated with N_2 at a pH 3, and he confirmed that the cleaning with the saturated CO_2 solution showed a higher cleaning efficiency. Although it was possible to examine the cleaning efficiency of the pH changes through an analysis of the cleaning efficiency in the inorganic fouling in the Partlan study, a pH effect is nonexistent because only organic fouling is caused in this experiment. Therefore, an increase of the cleaning efficiency in organic fouling is caused by a microbubble derived increase of the shear strength in the cleaning with the CO_2 injection.

The organic matter removal rates in the FOB with the injections of the dissolved air, N_2, and N_2 at a pH of 3.9 are similar to those of the existing FOB, 68.2%, 65.6%, and 68.5%, respectively, and the FOB with the dissolved CO_2 injection showed the highest organic matter removal efficiency of 82.5%.

Fig. 7 is a graph showing a comparison of the backwashingwater volume for each dissolved gas in the FOB. Although the backwashingwater volumes in the FOB with the injections of the dissolved air, N_2, and N_2 at a pH of 3.9 are similar to those of the existing FOB, the backwashingwater volume of the FOB with the dissolved CO_2 injection, 18.9 mL, is low. It is considered that the cleaning efficiency of the FOB can be lowered by widely forming a microbubble layer in the FOB to reduce the inflow of the backwashingwater from the generated microbubbles, but a cleaning efficiency that is higher than that of the existing FOB is shown by the enhanced shear strength result from the microbubbles.

Fig. 8 is a graph showing a comparison of after FOB reversible and irreversible resistances for each dissolved gas. The ratios are 35:65 for the injecting air-saturated solution, 36:64 for the injection of the N_2-saturated solution, and 29:71 for the injection of the N_2-saturated solution at the pH of 3.9.They are similar to those of the existing FOB. It was confirmed that the ratio is 48:52 for the injection of the CO_2-saturated solution and the reversible fouling proportion is high.

3.3. Cleaning efficiency according to the CO_2 injection method

This experiment compared the cleaning efficiency between the results of the existing FOB, the injection method of the CO_2, and according to the presence or absence of the FOB during the injection of the saturated CO_2. The velocities of the gas and the liquid during the injection of the CO_2 saturated solution were calculated as 0.0324 m/s and 0.0647 m/s, respectively. In addition, the gas and liquid velocities of the u_σ are 0.0458 m/s and 0.0915 m/s, respectively. Value θ, the gas/liquid ratio, is 0.5 and 0.33 for the injections of the non-dissolved CO_2 and the CO_2-saturated solution, respectively.

Fig. 9 is a graph showing a comparison of the cleaning efficiency and the organic matter removal rate for the CO_2 injection method of the FOB. The existing FOB showed a cleaning efficiency of 28%. And the FOB with the injection of the non-dissolved CO_2 showed a cleaning efficiency of 25.1%. The FOB with the injection of the CO_2-saturated solution showed a cleaning efficiency of 38.6%, without the performance of the FOB, it is 30.2%. It is considered that the cleaning efficiency was reduced by

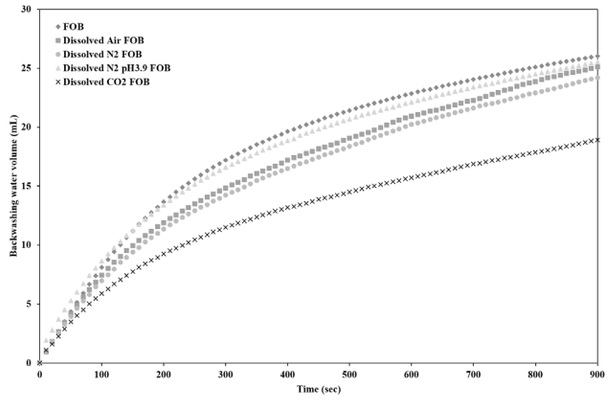

Fig. 7. Comparison of the back washing water volume for each gas of the FOB with the dissolved-gas injection.

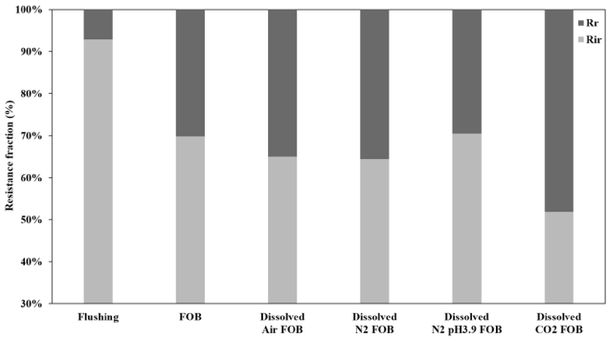

Fig. 8. Comparison of after FOB reversible and irreversible resistances for each gas with the dissolved-gas injection.

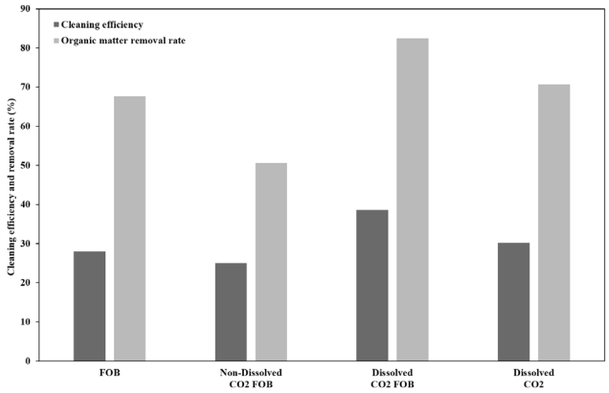

Fig. 9. Comparison of the cleaning efficiency and the organic matter removal rate for each CO_2-injection method of the FOB.

the low shear strength that is due to the relatively large bubble size during the injection of the CO_2 for which the non-dissolved gas-injection methods were used. And the microbubbles that were generated during the injection of the CO_2 saturated solution increased the cleaning efficiency with a higher shear strength. The high cleaning efficiency in the flushing for which the non-FOB performance CO_2 saturated solution was applied showed the foulant removal effect from a high shear strength, and it showed that the FOB performance makes it easier to remove irreversible fouling.

Cornelissen et al. reported that the bubble size became the same as that of the spacer grid in the narrow flow channel with the spacer during the injection of the non-dissolved gas [32]. Willems et al. also reported that bubbles of a similar size to the spacer were generated after a high speed camera measurement [31]. Drews et al. reported that the shear strength decreased with the increasing of the bubble size in the narrow-square flow channel with a 3 mm height, and the shear strength increased with the increasing of the bubble size in the relatively large-square flow channel with a height of 5–9 mm [33]. Chesters et al. reported that the cleaning efficiency was increased by the injection of the microbubbles in the chemical cleaning performance for the RO processes, and the cleaning efficiency increased with the decreasing of the bubble size [34]. Based on the results, the bubble size with the injection of the non-dissolved gas is larger than that with the injection of the CO_2-saturated solution. In addition, the experiment result was obtained with the use of the naked eye.

The organic matter removal efficiency in the existing FOB is 67.6%. And the FOB with the injection of the non-dissolved CO_2 showed an organic-matter removal efficiency of 50.7%. Although the FOB with the injection of the CO_2-saturated solution showed an organic matter removal efficiency of 82.5%, the organic matter removal efficiency without the FOB performance is 70.8%.

Fig. 10 is a graph showing a comparison of the backwashingwater volume for each of the CO_2-injection methods of the FOB. The backwashingwater volume in the existing FOB is 26 mL. However, the backwashingwater volumes in the FOB with the injection of the non-dissolved CO_2 and with the injection of the CO_2-saturated solution were reduced to 22.2 mL and 18.9 mL, respectively. It is considered that the backwashingwater volume was decreased because the microbubbles that were generated from the injection of the CO_2-saturated solution spread to all of the channels and interrupted the contact between the NaCl solution and the FOB-membrane surface.

Fig. 11 is a graph showing a comparison of after FOB reversible and irreversible resistances for each of the CO_2-injection methods. The ratios are 26:74 for the injection with the non-dissolved CO_2, 48:52 for the injection with the CO_2 saturated solution and the FOB, and 37:63 for the injection with the CO_2 saturated solution and without the FOB.

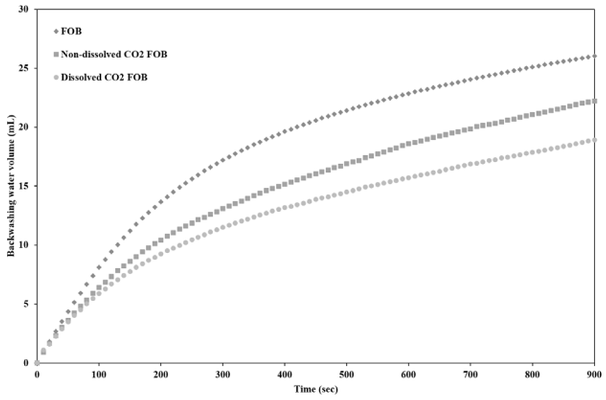

Fig. 10. Comparison of the backwashingwater volume for each CO_2-injection method of the FOB.

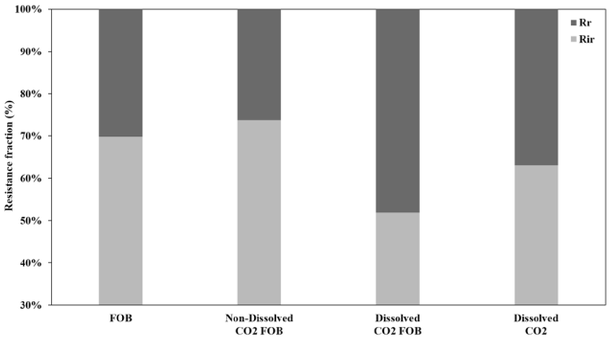

Fig. 11. Comparison of after FOB reversible and irreversible resistances for each CO_2-injection method of the FOB.

3.4. Cleaning efficiency according to the dissolved CO_2 pressure

In this experiment, the FOB was performed by inflowing the CO_2-saturated solution at a flow rate of 1 L/min for which the saturation pressure was changed from 100 kPa to 400 kPa. Table 2 shows the velocity and the gas/liquid ratio according to the dissolved CO_2 pressure. Fig. 12 is a graph showing the cleaning efficiency and the organic matter removal rate of the FOB according to the dissolved CO_2 pressure. The cleaning efficiencies are 38.6%, 43.6%, 35.7%, and 34.4% at pressures of 100 kPa, 200 kPa, 300 kPa, and 400 kPa, respectively. The highest cleaning efficiency is at the pressure of 200 kPa. It is considered that this was caused by a gas/liquid ratio of θ because the results were obtained under the same influent pressure and flow rate. The value θ is 0.49 at a dissolved pressure of 200 kPa, and the gas/liquid ratio is 1:1.

Ducom et al. reported that the shear strength was increased in proportion to the gas ratio when the gas and liquid flows occurred at the same time [35,36]. Cornelissen et al. reported that the cleaning efficiencies varied depending on the air/water ratio in terms of an application of air flushing to spiral-wound membranes; furthermore, the cleaning efficiencies are the highest with an air/water ratio of 4:1 [32]. Wibisono, however, reported that the bubble size increased with the increasing of the gas ratio in the flow channel with the spacers [28]. In addition, the gas/liquid ratio with the optimal cleaning efficiency should vary because the solubility of CO_2 is higher than that of air.

The organic matter removal rates are 82.5%, 84.2%, 72.0%, and 73.4% at the pressures of 100 kPa, 200 kPa, 300

Table 3
Changes in the velocity according to the dissolved CO_2 pressure

Dissolved pressure (kPa)	Gas velocity, u_G (m/s)	Liquid velocity, u_L (m/s)	Gas velocity vector, $u_G\sigma$ (m/s)	Liquid velocity vector, $u_L\sigma$ (m/s)	Gas/Liquid ratio, θ
100	0.0324	0.0647	0.0458	0.0915	0.33
200	0.0472	0.0498	0.0668	0.0705	0.49
300	0.0589	0.0382	0.0833	0.0540	0.61
400	0.0692	0.0278	0.0979	0.0393	0.71

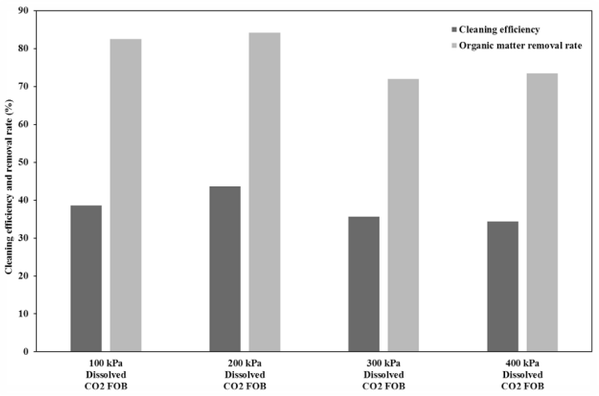

Fig. 12. Comparison of the cleaning efficiency and the organic-matter removal rate for each dissolved CO_2 pressure of the FOB.

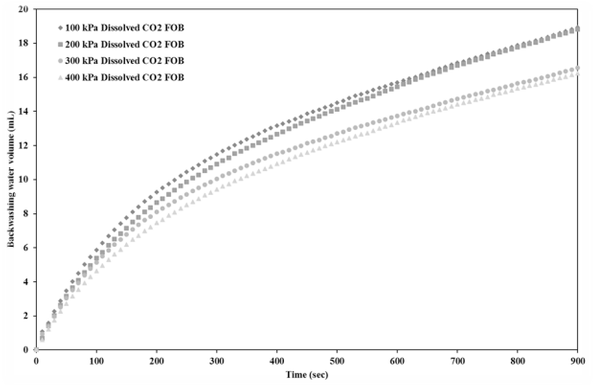

Fig. 13. Comparison of the backwashing-water volume for each dissolved CO_2 pressure of the FOB.

kPa, and 400 kPa, respectively. The highest efficiency of the organicmatter removal was found at the pressure of 200 kPa.

Fig. 13 is a graph showing a comparison of the backwashing-water volume for each of the dissolved CO_2 pressures of the FOB. The backwashingwater volumes are 18.9 mL, 18.8 mL, 16.6 mL, and 16.2 mL at the pressures of 100 kPa, 200 kPa, 300 kPa, and 400 kPa, respectively. Although the backwashing-water volumes at the pressures of 100 kPa and 200 kPa are not majorly different, a slightly decreasing tendency at the pressures of 300 kPa and 400 kPa is evident. The backwashingwater volume decreased with the increasing of the gas/liquid ratio via the interruption of the contact between the NaCl solution and the membrane surface. The backwashingwater volumes at the pressures of 100 kPa and 200 kPa are similar. It is considered that the interruption of the contact between the NaCl solution and the membrane surface was minimized by the disturbance of the microbubbles, because the interaction between the gas and the liquid is ideal with the value θ of 0.5.

Fig. 14 is a graph showing a comparison of the reversible and irreversible resistances for each dissolved CO_2 pressure. The ratios of the reversible and irreversible resistances are 48:52, 49:51, 39:61, and 38:62 at the pressures of 100 kPa, 200 kPa, 300 kPa, and 400 kPa, respectively. The highest reversibility was found at a pressure of 200 kPa, and the irreversible fouling is high at the pressures of 300 kPa and 400 kPa.

Fig. 15 is a graph showing a comparison of the cleaning efficiencies and the backwashing-water volumes for each

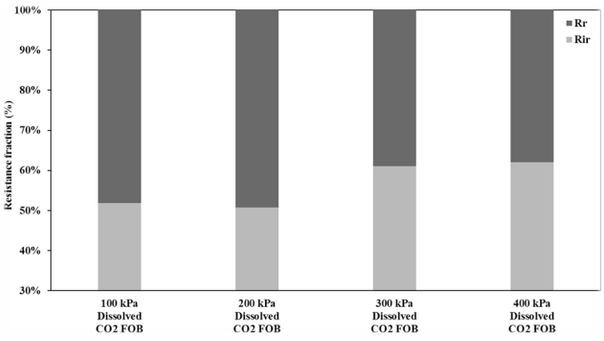

Fig. 14. Comparison of the post-FOB reversible and irreversible resistances for each dissolved-CO_2 pressure of the FOB.

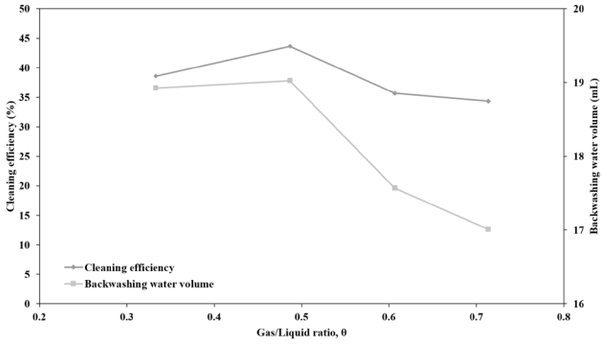

Fig. 15. Comparison of the cleaning efficiency and the backwashing water volume for each gas/liquid ratio.

ratio of the CO_2 and NaCl solutions. The highest cleaning efficiency was found at the value θ of 0.49. It was confirmed that the cleaning efficiencies and the backwashing-water volumes decreased with the increasing of the value θ.

4. Conclusion

In this study, the following conclusions were drawn through a comparison and evaluation of the cleaning efficiencies according to the conditions during the FOB performance for which gas flushing is applied during the RO processes for high-salinity wastewater.

The FOB showed lower efficiencies than the existing FOB when the non-dissolved gas was injected. The gas flown to the flow channel in the feed side forms gas layers due to the relatively low velocity, and an effective turbulence is not formed. Moreover, the generated gas layers reduced the cleaning efficiencies by interrupting the contact between the NaCl solution and the membrane surface and the inflow of the backwashingwater in the FOB.

Although the N_2 and air did not generate bubbles due to a low solubility during the injection of the dissolved gas, the CO_2 showed higher cleaning efficiencies than the existing FOB by generating high solubility based microbubbles. The cleaning efficiencies of the FOB for which the N_2saturated solution that had been lowered to a pH of 3.9 was used did not change because the pH was decreased when the CO_2 was dissolved. Based on the results, the physical microbubble effects are more dominant than those of the pH in the CO_2 cleaning.

This study evaluated the cleaning efficiencies according to the CO_2injection method. As a result, the microbubbles that were generated by the injection of the CO_2 saturated solution showed higher cleaning efficiencies due to the characteristics of the RO membrane modules in the narrow flow channel with the spacer. The highest cleaning efficiency was found when the CO_2 cleaning and the FOB were performed at the same time.

This study evaluated the cleaning efficiencies according to the dissolved CO_2 pressure. As a result, the amount of generated gas was increased with the increasing of the dissolved pressure. Accordingly, the value θ as the gas/liquid ratio was increased with the increasing of the pressure. In particular, the highest cleaning efficiency was found at the pressure of 200 kPa, and the value θ was increased to 0.49 in this case. It was confirmed that the ideal cleaning was realized when the ratio of the CO_2/NaCl solution is 1:1. Based on the results of the present study, it is necessary to select the proper dissolved CO_2 pressure. It is consider that it is possible to perform the CO_2 cleaning at a relatively low cost compared with air-generated microbubbles method.

Acknowledgments

This research was supported by a grant (code 17IFIP-C088924-04) from Industrial Facilities & Infrastructure Research Program funded by Ministry of Land, Infrastructure and Transport (MOLIT) of the Korea government and the Korea Agency for Infrastructure Technology Advancement (KAIA).

References

[1] M.A. Shannon, P.W. Bohn, M. Elimelech, J.G. Georgiadis, B.J. Marinas, A.M. Mayes, Science and technology for water purification in the coming decades, Nature, 452 (2008) 301–310.
[2] S. Gray, R. Semiat, M. Duke, A. Rahardianto, Y. Cohen, 4.04 - Seawater Use and Desalination Technology A2 - Wilderer, Peter, in: Treatise on Water Science, Elsevier, Oxford, 2011, pp. 73–109.
[3] O. Lefebvre, R. Moletta, Treatment of organic pollution in industrial saline wastewater: A literature review, Water Res., 40 (2006) 3671–3682.
[4] C. Sun, T. Leiknes, J. Weitzenböck, B. Thorstensen, Development of an integrated shipboard wastewater treatment system using biofilm-MBR, Separ. Purif. Technol., 75 (2010) 22–31.
[5] J.P. Bassin, R. Kleerebezem, G. Muyzer, A.S. Rosado, M.C. van Loosdrecht, M. Dezotti, Effect of different salt adaptation strategies on the microbial diversity, activity, and settling of nitrifying sludge in sequencing batch reactors, Appl. Microbiol. Biotechnol., 93 (2012) 1281–1294.
[6] J. Hong, W. Li, B. Lin, M. Zhan, C. Liu, B.-Y. Chen, Deciphering the effect of salinity on the performance of submerged membrane bioreactor for aquaculture of bacterial community, Desalination, 316 (2013) 23–30.
[7] C. Fritzmann, J. Löwenberg, T. Wintgens, T. Melin, State-of-the-art of reverse osmosis desalination, Desalination, 216 (2007) 1–76.
[8] M. Elimelech, W.A. Phillip, The future of seawater desalination: energy, technology, and the environment, Science, 333 (2011) 712–717.
[9] L.F. Greenlee, D.F. Lawler, B.D. Freeman, B. Marrot, P. Moulin, Reverse osmosis desalination: water sources, technology, and today's challenges, Water Res., 43 (2009) 2317–2348.
[10] N. Ghaffour, T.M. Missimer, G.L. Amy, Technical review and evaluation of the economics of water desalination: Current and future challenges for better water supply sustainability, Desalination, 309 (2013) 197–207.
[11] W. Arras, N. Ghaffour, A. Hamou, Performance evaluation of BWRO desalination plant — A case study, Desalination, 235 (2009) 170–178.
[12] J.P. Chen, S.L. Kim, Y.P. Ting, Optimization of membrane physical and chemical cleaning by a statistically designed approach, J. Membr. Sci., 219 (2003) 27–45.
[13] J.W. Nam, J.Y. Park, J.H. Kim, Y.S. Lee, E.J. Lee, M.J. Jeon, H.S. Kim, A. Jang, Effect on backwash cleaning efficiency with TDS concentrations of circulated water and backwashingwater in SWRO membrane, Desal. Water Treat., 43 (2012) 124–130.
[14] J.-J. Qin, M.H. Oo, K.A. Kekre, B. Liberman, Development of novel backwash cleaning technique for reverse osmosis in reclamation of secondary effluent, J. Membr. Sci., 346 (2010) 8–14.
[15] J. Vrouwenvelder, D. Van der Kooij, Diagnosis, prediction and prevention of biofouling of NF and RO membranes, Desalination, 139 (2001) 65–71.
[16] E. Cornelissen, J. Vrouwenvelder, S. Heijman, X. Viallefont, D. Van Der Kooij, L. Wessels, Periodic air/water cleaning for control of biofouling in spiral wound membrane elements, J. Membr. Sci., 287 (2007) 94–101.
[17] M. Fazel, S. Chesters, RO membrane cleaning using microbubbles at 6,800 m^3/d wastewater RO plant in UAE, Desal. Water Treat., 55 (2015) 3358–3366.
[18] Z. Cui, T. Taha, Enhancement of ultrafiltration using gas sparging: a comparison of different membrane modules, J. Chem. Technol. Biotechnol., 78 (2003) 249–253.
[19] I.S. Ngene, R.G. Lammertink, A.J. Kemperman, W.J. van de Ven, L.P. Wessels, M. Wessling, W.G. Van der Meer, CO_2 nucleation in membrane spacer channels remove biofilms and fouling deposits, Ind. Eng. Chem. Res., 49 (2010) 10034–10039.
[20] E. Partlan, Dissolved Carbon Dioxide for Scale Removal in Reverse Osmosis, 2013.
[21] A. Sagiv, N. Avraham, C.G. Dosoretz, R. Semiat, Osmotic backwash mechanism of reverse osmosis membranes, J. Membr. Sci., 322 (2008) 225–233.

[22] N. Avraham, C. Dosoretz, R. Semiat, Osmotic backwash process in RO membranes, Desalination, 199 (2006) 387–389.
[23] A. Sagiv, R. Semiat, Backwash of RO spiral wound membranes, Desalination, 179 (2005) 1–9.
[24] A. Sagiv, R. Semiat, Modeling of backwash cleaning methods for RO membranes, Desalination, 261 (2010) 338–346.
[25] A. Sagiv, R. Semiat, Parameters affecting backwash variables of RO membranes, Desalination, 261 (2010) 347–353.
[26] M.H. Sharqawy, J.H. Lienhard, S.M. Zubair, Thermophysical properties of seawater: a review of existing correlations and data, Desal. Water Treat., 16 (2010) 354–380.
[27] A.W. Islam, E.S. Carlson, Viscosity models and effects of dissolved CO_2, Energy Fuels, 26 (2012) 5330–5336.
[28] Y. Wibisono, Two-phase flow for fouling control in membranes, Universiteit Twente, 2014.
[29] A. Da Costa, A. Fane, D. Wiley, Spacer characterization and pressure drop modelling in spacer-filled channels for ultrafiltration, J. Membr. Sci., 87 (1994) 79–98.
[30] T. Wilmarth, M. Ishii, Two-phase flow regimes in narrow rectangular vertical and horizontal channels, Int. J. Heat Mass Transfer, 37 (1994) 1749–1758.
[31] P. Willems, A. Kemperman, R. Lammertink, M. Wessling, M. van Sint Annaland, N. Deen, J. Kuipers, W. Van der Meer, Bubbles in spacers: Direct observation of bubble behavior in spacer filled membrane channels, J. Membr. Sci., 333 (2009) 38–44.
[32] E. Cornelissen, L. Rebour, D. Van der Kooij, L. Wessels, Optimization of air/water cleaning (AWC) in spiral wound elements, Desalination, 236 (2009) 266–272.
[33] A. Drews, H. Prieske, E.-L. Meyer, G. Senger, M. Kraume, Advantageous and detrimental effects of air sparging in membrane filtration: Bubble movement, exerted shear and particle classification, Desalination, 250 (2010) 1083–1086.
[34] S.P. Chesters, M.W. Armstrong, M. Fazel, Microbubble RO membrane cleaning reduces fouling on WWRO plant, Desal. Water Treat., 55 (2015) 2900–2908.
[35] G. Ducom, F. Puech, C. Cabassud, Air sparging with flat sheet nanofiltration: a link between wall shear stresses and flux enhancement, Desalination, 145 (2002) 97–102.
[36] G. Ducom, F.P. Puech, C. Cabassud, Gas/liquid two-phase flow in a flat sheet filtration module: measurement of local wall shear stresses, Canad. J. Chem. Eng., 81 (2003) 771–775.